

Utah State University

DigitalCommons@USU

Space Dynamics Lab Publications

Space Dynamics Lab

1-1-1973

Rocket-Borne Radiometric Measurements of OH in the Auroral Zone

J. W. Rogers

R. E. Murphy

A. T. Stair Jr.

J. C. Ulwick

Follow this and additional works at: https://digitalcommons.usu.edu/sdl_pubs

Recommended Citation

Rogers, J. W.; Murphy, R. E.; Stair, A. T. Jr.; and Ulwick, J. C., "Rocket-Borne Radiometric Measurements of OH in the Auroral Zone" (1973). *Space Dynamics Lab Publications*. Paper 112.

https://digitalcommons.usu.edu/sdl_pubs/112

This Article is brought to you for free and open access by the Space Dynamics Lab at DigitalCommons@USU. It has been accepted for inclusion in Space Dynamics Lab Publications by an authorized administrator of DigitalCommons@USU. For more information, please contact digitalcommons@usu.edu.



Rocket-borne Radiometric Measurements of OH in the Auroral Zone

J. W. ROGERS, R. E. MURPHY, A. T. STAIR, JR., AND J. C. ULWICK

Air Force Cambridge Research Laboratories, Bedford, Massachusetts 01730

K. D. BAKER AND L. L. JENSEN

Utah State University, Logan, Utah 84321

An Astrobee D rocket carrying a dual-channel radiometer (1.40- to 1.65- μm and 1.85- to 2.12- μm spectral band passes) was launched on March 6, 1972, at 0200 LT from Poker Flat, Alaska. The spectral band passes were chosen so that the lower ($\nu = 2, 3, 4, 5$) and upper ($\nu = 7, 8, 9$) vibrational levels of OH in the $\Delta\nu = 2$ sequence could be monitored simultaneously. Launch criteria were established from ground-based radiometric observations that indicated a steady night airglow of 240 kR in the 1.40- to 1.65- μm band pass 2 hours prior to and throughout the flight. Altitude profiles of OH emission were derived from data from both channels and show OH to be layered, peak volume emissions occurring at 83.5 km. Under the assumption that $\text{H} + \text{O}_3 \rightarrow \text{OH}^\dagger + \text{O}_2$ is the principal production mechanism, synthetic spectra were integrated over the instrument spectral response characteristics of the two radiometer channels. At altitudes above 83 km, quenching due to the reaction $\text{OH}^\dagger + \text{O} \rightarrow \text{O}_2 + \text{H}$ is evident, which requires an atomic oxygen concentration of 10^{11} cm^{-3} at 83 km, increasing to $8 \times 10^{11} \text{ cm}^{-3}$ at 88 km.

Over the past two decades, considerable speculation on the origin of hydroxyl emission and the hydrogen-oxygen chemistry in the upper atmosphere has been offered [Bates and Moisewitsch, 1956; Krassovsky *et al.*, 1961; Krassovsky, 1971]. These speculations have been accompanied by a number of hydroxyl measurements taken with ground-based, balloon-borne, and rocket-borne instruments [Gush and Buijs, 1964; Baker and Waddoups, 1967; Shefov, 1971, 1972; Bunn and Gush, 1972; Lowe and Lytle, 1973] concerned with specific details of the overall phenomena. Unfortunately, substantial uncertainty remains concerning the processes that govern the OH emission, particularly in the auroral zone where enhanced emissions have been recorded [Stair *et al.*, 1971]. Rocket measurements to determine the altitude distributions for different vibrational levels during different times of the day are essential to determine the various mechanisms that control the degree of excitation of OH in the atmosphere [Shefov, 1972].

A rocket-borne simultaneous measurement of the upper and lower vibrational levels of OH in the first overtone ($\Delta\nu = 2$ sequence) was

conducted from Poker Flat, Alaska, on March 6, 1972. The simultaneous monitoring of the emission from lower vibrational levels together with the measurements of the upper vibrational levels may provide information on quenching, radiative cascade, and other production mechanisms. Measurements of the emission from the upper vibrational levels were made to determine the contribution due to the $\text{H} + \text{O}_3$ reaction.

At altitudes above 83 km the emission from the lower vibrational levels with respect to the measurement of the upper vibrational levels is less than the calculated value for OH production from $\text{H} + \text{O}_3$ and radiative cascade. This result has been interpreted as being due to quenching of OH by reaction with atomic oxygen. On the basis of OH being quenched, atomic oxygen concentrations have been determined and compared with other measurements. At altitudes below 82 km the data indicate that the $\text{H} + \text{O}_3$ reaction by itself is apparently not adequate to account for the emission from the lower vibrational levels.

INSTRUMENTATION

A spin-stabilized Astrobee D rocket (A30.205-3) was launched from Poker Flat, Alaska, on

March 6, 1972 at 1214 UT (0214 LT). The rocket carried a pay load of about 30 lb to a peak altitude of 89.4 km in approximately 145 sec. Total rocket flight time was about 330 sec, and the rocket impacted 57 km north (magnetic) of the rocket launch site. The tip of the rocket was ejected at 53.5 sec (50-km altitude) to expose the infrared sensor, which was a liquid nitrogen cooled dual-channel radiometer. Tip-over and loss of usable data occurred at 190 sec or approximately 81 km on the downleg. Altitude was determined by ground-based tracking, and the error is less than 0.5 km.

An aspect magnetometer was mounted perpendicular to the longitudinal axis of the rocket and provided data on rocket roll rate (spin) as well as rocket cone angle relative to the earth's magnetic field. As was indicated by the magnetometer, the rocket achieved a relatively constant roll rate of 8 revolutions per second, and the precessional motion (37-sec period) gave rise to a minimum-maximum look angle of about 2° – 25° from the vertical.

The primary sensor in the pay load was a newly developed dual-channel liquid nitrogen cooled radiometer [Jensen *et al.*, 1972] for measurement of hydroxyl emissions. The radi-

ometer (Figure 1) contained separate detectors (InSb) and optical components for each channel and shared a common chopper housed in a cryogenic liquid nitrogen dewar. The spectral band-pass filter for the short-wavelength channel, 1.40–1.65 μm (half power points), was chosen to accept emission from the 2-0 through 5-3 vibration-rotation bands of OH. The longer-wavelength channel covered 1.85–2.12 μm corresponding to the 7-5 through 9-7 vibration-rotation bands. The fields of view were 10° full cone angles, and the viewing direction of both channels was 0° relative to the rocket forward axis. A cold cover sealed the optical components until tip ejection at 50 km.

MEASUREMENTS

The rocket launch criterion established for this experiment was a moderate nighttime sky with respect to OH enhancement. Ground-based measurements of the 3914-A N_2^+ (1 N) and 5577-A $\text{O}(\text{S})$ lines from the regions near the rocket trajectory showed the general auroral conditions prior to and during the rocket flight to be rather weak, a few kR [Huppi *et al.*, 1973], at the launch site. These conditions assured no measurable signal in the infrared

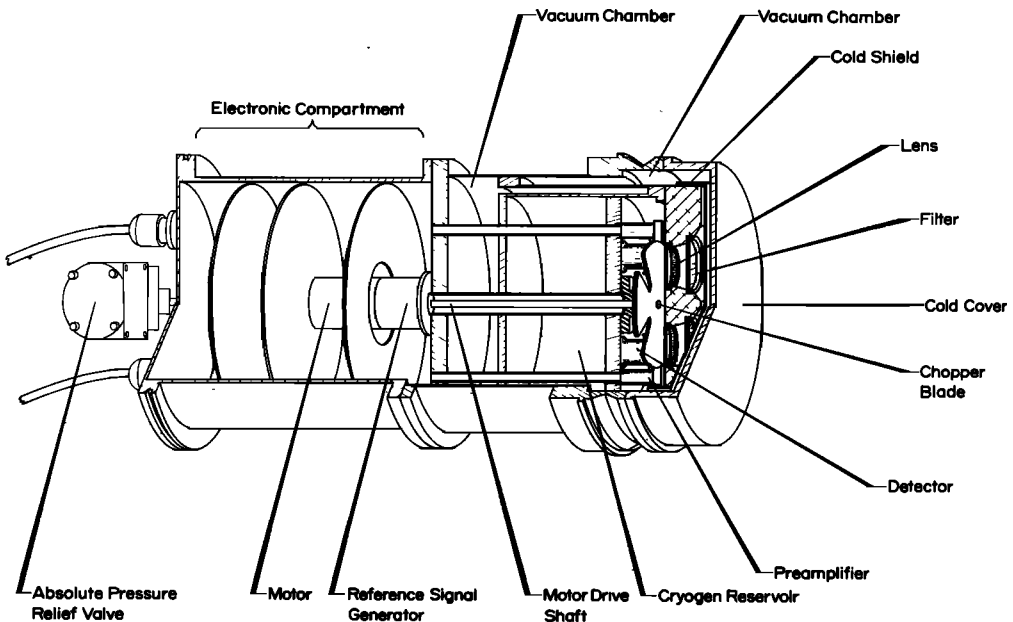


Fig. 1. Dual-channel radiometer. Spectral filters covering $\Delta\nu = 2$ sequence of OH, short wavelength 1.40–1.65 μm , ($\nu-\nu$) 2-0, 3-1, 4-2 and 5-3. Long wavelength 1.85–2.12 μm , ($\nu-\nu$) 7-5, 8-6 and 9-7.

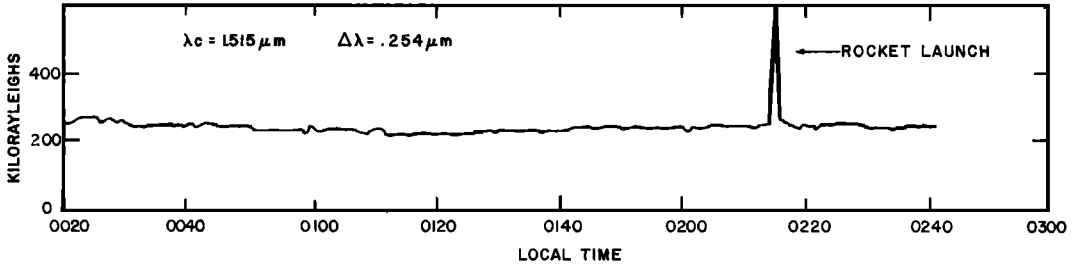


Fig. 2. Ground-based radiometric measurements, March 6, 1972, where λ_c is the center of the band pass [Huppi *et al.*, 1973]. The spectral band pass was almost identical to that of the lowest wavelength channel of the rocket-borne radiometer.

due to nitrogen fluorescence. In addition, a ground-based radiometer having the same spectral band pass as the short-wavelength channel radiometer on board the rocket was monitored before and during the flight. The ground-based OH radiometer indicated steady OH emission (10% slow variation) 1 hour before launch and a steady 240-kR emission just prior to launch until after the flight [Huppi *et al.*, 1973] (Figure 2).

Telemetry data were digitized every 2 msec and processed by a digital computer. Figure 3 shows the radiance in MR as a function of rocket altitude for the two radiometer channels. The data points shown have been averaged approximately every $\frac{1}{2}$ km. To minimize the

effect of rocket spin, each computed point has an integral number of rocket revolutions. The open circles and squares represent data points taken on the upleg of the flight, whereas the solid circles and squares are data points obtained during descent. The horizontal bars are one standard deviation about each data point. As the figure shows, the scatter in the data is smaller at higher altitudes. The magnitude of scatter is related to the integration time; that is, the vertical velocity of the rocket is decreasing, and the observation time is constantly increasing with altitude, from $\frac{1}{2}$ sec at 75 km to 7 sec at 88 km. The standard deviation for the short-wavelength channel varies from 8 kR at 73 km to 2 kR at 88 km. The long-wave-

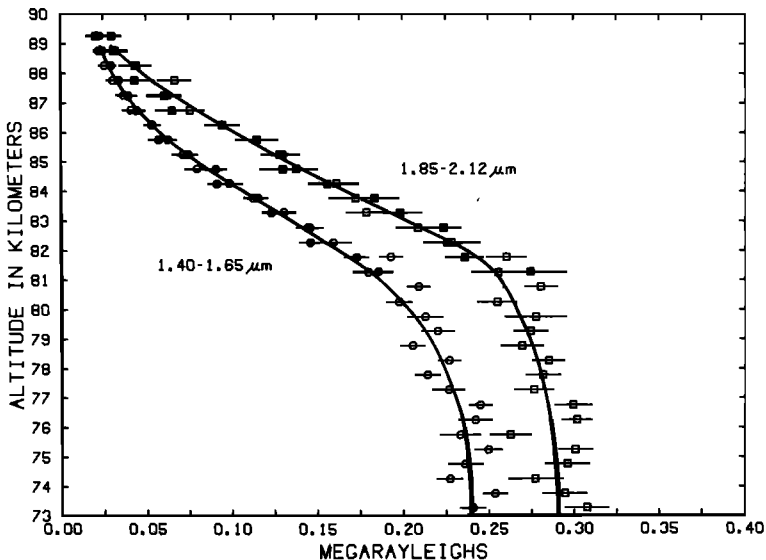


Fig. 3. Corrected integrated OH emission versus rocket altitude. Open data points and solid data points represent the upleg and the downleg of the rocket flight, respectively. The curves are obtained by smoothing the data with a Gaussian weight. The horizontal bars are one standard deviation about each data point.

length channel had standard deviations that varied from 13 to 6 kR. The effect of rocket tip-over is also obvious in the raw data before correction for aspect. The magnetometer data show that rocket tip-over begins at about 190 sec (apogee at 145 sec). At 207 sec (70-km altitude) the longitudinal axis of the rocket is perpendicular to the magnetic field. Consequently, data obtained on the downleg are limited to altitudes greater than 81 km in order to keep the slant path less than 25° from the vertical. The aspect determination assumes that the axis of precession lies in the plane of the earth's magnetic field. These data have been corrected in accordance with the magnetometer data to correspond to a vertical look angle by using a cosine slant path. The solid curve is a result of smoothing the data points with a Gaussian weight [Pearce, 1969]. The weighting interval was chosen to be proportional to the standard deviation of the data at the altitude of calculation and varied from 6 to 1.5 km. This criterion was chosen because less smoothing was desired where the data are more reliable.

RESULTS AND DISCUSSION

The signal in both channels of the radiometer approaches zero at apogee, indicating that the

majority of the emitting OH layer has been traversed by the rocket. In the 1.40- to 1.65- μm spectral region the ground-based measurements and rocket data below 70 km indicate good agreement, both measuring 230–240 kR. This implies that the majority of the emission occurs at altitudes above 70 km, in agreement with current models for postlocal midnight [Shimazaki and Laird, 1970; Gattinger, 1969, 1971], since OH production at lower altitudes decreases after sunset owing to the rapid recombination of atomic oxygen and hydrogen.

The reliability of the data was further established by digitizing the response-corrected spectrum of Gush and Buijs [1964] and integrating it with the rocket instrument response. The ratio of the high-wavelength channel to the low-wavelength channel obtained by using their data is 1.2. This is in good agreement with the data obtained from the rocket below 75 km.

Figure 4 shows the volume emission rates that were obtained by differentiation of the data, again by means of a Gaussian weight [Pearce, 1969], as a function of altitude. The curve has been drawn as a dashed line below 79 km to indicate that the accuracy of the derivative is questionable owing to the larger uncertainties in the original data at these altitudes. The maximum volume emission rates in

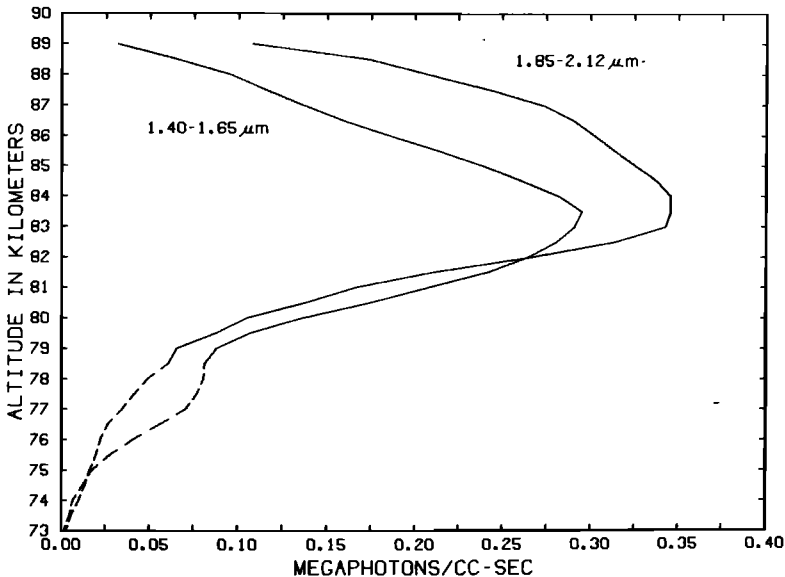


Fig. 4. OH volume emission profiles derived from the derivatives of radiometric measurements of the $\Delta\nu = 2$ sequence in the spectral bands indicated. The curves are dashed below 79 km because of the uncertainties in the original data.

the short- and long-wavelength channels are 2.9×10^5 and 3.5×10^5 photons/cm³ sec. It is seen that the OH emission is concentrated in a layer at 83.5 km approximately 8 km in depth. Both the altitude distribution and absolute rates are in agreement with the midnight model of *Gattinger* [1971], which shows a total OH peak rate of about 1.4×10^6 photons/cm³ sec at about 82 km. *Baker* [1967] and *Harrison* [1971] have measured peak volume emission rates at approximately 95 km, whereas *Packer* [1961] and *Tarasova* [1963] have obtained peak emission at 80–85 km. At altitudes below 82 km the emission rate in the short-wavelength channel exceeds that of the long-wavelength channel. At these altitudes, minor constituents change dramatically, and, if two or more processes are operative to a significant extent, it is likely that the volume emission rates from different processes would be in evidence.

It is generally conceded that the reaction



is one of the dominant production mechanisms of vibrationally excited hydroxyl in the upper atmosphere. From laboratory studies it has been established that reaction 1 populates preferentially in $v = 8$ and 9 [*Charters et al.*, 1971]. The spectral band pass of the long-wavelength channel was chosen to encompass only the higher vibrational emissions of the $\Delta v = 2$ sequence; consequently, the contribution from reaction 1 can be established, and the amount of radiation falling in the short-wavelength channel due to reaction 1 can be calculated and compared with the measured values.

Synthetic emission spectra of the $\Delta v = 2$ sequence of OH were generated in accordance with

$$I_{\nu, J' J''} \propto N_{\nu, J'} h\nu_{\nu, J' J''} A_{\nu, \nu'} S_{J' J''} \quad (2)$$

where $\nu_{\nu, J' J''}$ is the frequency of radiation resulting from the transition from vibrational state ν' to ν and rotational state J' to J , $A_{\nu, \nu'}$ is the vibrational transition probability, $S_{J' J''}$ is the rotational line strength, and $N_{\nu, J'}$ is the relative population in levels ν' and J' . The rotational population was taken as a Boltzmann distribution at 200°K to correspond to a midnight-winter atmosphere [*Sivjee et al.*, 1972]. Ther-

mally averaged (200°K) vibrational transition probabilities based on an ab initio calculation were used (F. H. Mies, private communication, 1973). These probabilities are in agreement with the experimentally measured intensities I_{20}/I_{21} and I_{31}/I_{32} of *Murphy* [1971] and should be more reliable for transitions involving higher vibrational quantum numbers, since more accurate wave functions were used in the calculations. The relative vibrational population was obtained by solving the equilibrium flux equation

$$\frac{dN_{\nu}}{dt} = 0 = F_{\nu} + \sum_{\nu'=v+1}^9 N_{\nu'} A_{\nu'} \nu' - N_{\nu} \sum_{\nu''=0}^{v-1} A_{\nu''} \nu \pm Q_{\nu} (v = 1-9) \quad (3)$$

where the terms on the right represent the initial production rate of OH into level ν by the reaction $\text{H} + \text{O}_3$, determined from the experiment by *Charters et al.* [1971] at a pressure of 10^{-4} torr and corrected with the vibrational transition probabilities of F. H. Mies (private communication, 1973), the rate of excited OH molecules cascading by radiation into level ν from higher levels ν' , the loss rate of excited OH molecules from level ν by radiation, and the loss rate (or gain) of OH molecules from level ν by quenching (or mechanisms other than $\text{H} + \text{O}_3$).

The synthetic emission spectrum for the first overtone of OH was calculated by using (2) and (3) with Q_{ν} initially set at zero. This spectrum was integrated with the instrument response of the two-wavelength channels. The computed intensity ratio R_c of the 1.40- to 1.65- μm region of the spectrum to the 1.85- to 2.12- μm region of the spectrum is 0.97.

The ratio of the volume emission rates for the two data channels as a function of altitude is presented in Figure 5. The measured intensity ratios R_m are compared to the intensity ratio R_c calculated from the theoretical spectra integrated with the response of the two data channels.

Based on the $\text{H} + \text{O}_3$ reaction's being the sole source of vibrationally excited hydroxyl, the calculated ratio R_c indicates that there should be 0.97 times as much radiation in the long-wavelength data channel as there is in the short-wavelength data channel if it is assumed

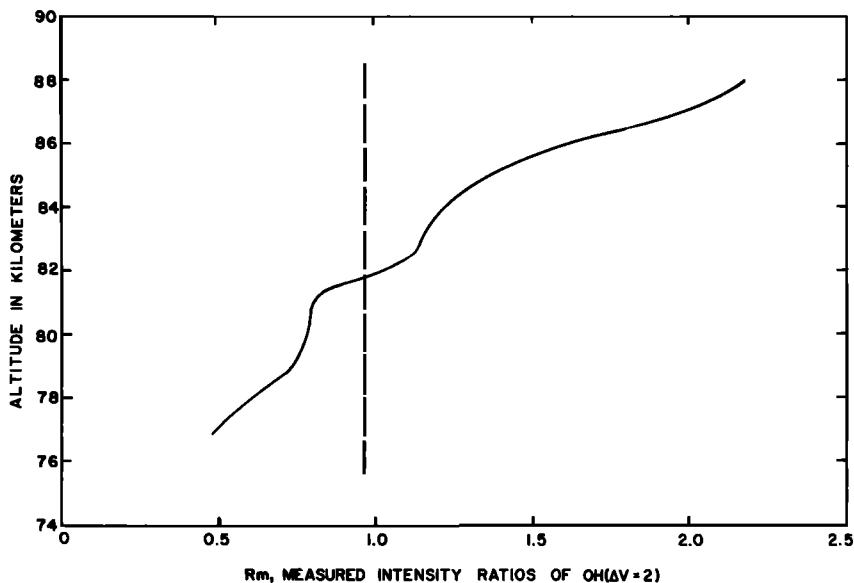


Fig. 5. The measured intensity ratios of OH ($\Delta v = 2$ sequence) for the two radiometric channels as a function of altitude. The dashed line represents the expected ratio for the $H + O_3$ reaction alone with radiative cascade and no quenching.

that there is no quenching of OH. The measured ratios (Figure 5) show that this condition is met at approximately 82 km. Relative to the long-wavelength data channel, the short-wavelength data channel has a larger emission below 82 km and a smaller emission above 82 km than is predicted by the calculated ratio R_c . Below 82 km this is an indication of possible additional processes producing excited OH in lower vibrational levels [Krassovsky, 1971].

At altitudes greater than 82 km, quenching of vibrationally excited hydroxyl may be important. Quenching of OH by the dominant species N_2 or O_2 may be excluded [Worley *et al.*, 1971, 1972]. However, chemical reaction with atomic oxygen is very fast, the rate constant being reported at $5 \pm 2 \times 10^{-11} \text{ cm}^3 \text{ sec}^{-1}$ [Kaufman, 1964], but no information is available on the rate constant as a function of the vibrational state of OH.

Since the rate constant may be vibrationally dependent, an empirical relation for the vibrational quenching of OH was assumed.

$$Q_v = k(1 + \alpha v)[O][N_v] \quad (4)$$

The linear dependence of the rate constant on v must be small, since the reaction rate is very near gas kinetic [Kaufman, 1964]. If the reac-

tion rate is assumed to vary from $5 \times 10^{-11} \text{ cm}^3 \text{ sec}^{-1}$ for the lowest vibrational level to $10^{-10} \text{ cm}^3 \text{ sec}^{-1}$ for the ninth vibrational level [Krassovsky, 1973], a value of 0.11 is obtained for α .

After introducing (4) into the right side of (3), vibrational distributions were calculated for various atomic oxygen concentrations. These populations were incorporated into (2) to generate theoretical spectra, which were then integrated with the response of each data channel. These calculated ratios R_c of the long-wavelength data channel to the short-wavelength data channel are determined as a function of altitude and are shown in Figure 6. Both curves in Figure 6 use the OH production rates based on the experiments of Charters *et al.* [1971], corrected by the vibrational transition probabilities of F. H. Mies (private communication, 1973). The solid curve was obtained by using $\alpha = 0.11$ in (4) and illustrates the case of vibrationally dependent quenching. The dashed curve with $\alpha = 0$ shows the results for a vibrationally independent quenching rate.

From the measured intensity ratios R_m as a function of altitude (Figure 5) and the computed intensity ratios R_c as a function of $[O]$ (Figure 6) an atomic oxygen profile was determined (Figure 7). The dashed curves show the

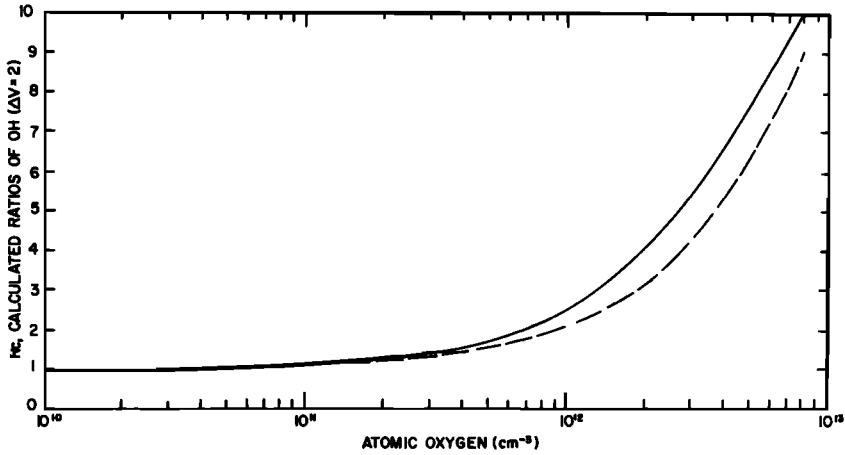


Fig. 6. The calculated intensity ratios of OH ($\Delta v = 2$ sequence) for the two radiometric channels as a function of atomic oxygen concentration. The solid curve represents a vibrationally dependent quenching rate, and the dashed curve represents a vibrationally independent quenching rate.

limits based on the most probable error. The atomic oxygen profile of *Henderson* [1971], measured during the daytime at Wallops Island, is shown by the dotted curve.

From a nighttime auroral zone rocket measurement of the 5577 O(¹S) emission, *Dandekar* [1972] has derived an atomic oxygen profile.

He concludes that the peak atomic oxygen concentration occurs at a significantly lower altitude in the auroral zone than indicated by the lower latitude observations and theoretical profiles. Two values are quoted by *Dandekar* depending on the model origin of the O(¹S) emission. Although the absolute atomic oxygen

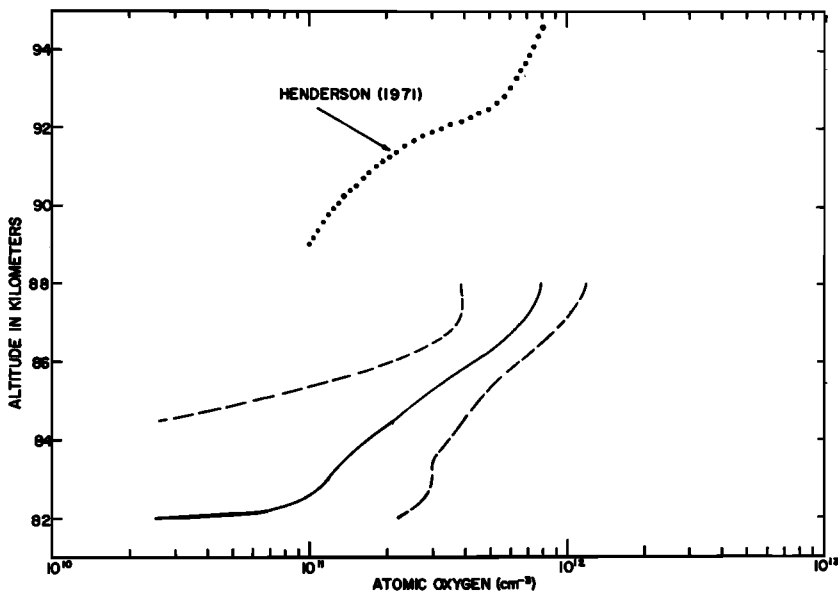


Fig. 7. Derived atomic oxygen concentrations from the OH volume emission profiles using a vibrationally dependent quenching rate. The dashed curves show the limits based on the most probable error. The dotted curve is a measurement by *Henderson* [1971] obtained during the daytime at Wallops Island.

concentration varies depending on the model origin, the peak of both profiles occurs around 86 km, which is consistent with the present measurement.

In view of the altitude conclusions of *Dandekar* [1972] and subject to the uncertainties in the vibrational production rates of OH from $H + O_3$ and the vibrational quenching rate for $OH^{\ddagger} + O$, the agreement of the atomic oxygen profile with current models [*Shimazaki and Laird*, 1970] is satisfying.

Evans and Llewelyn [1971] have indicated that measurements from a balloon-borne instrument [*Bunn and Gush*, 1972] show no indication of atomic oxygen quenching. It appears that the small degree of quenching observed on this rocket flight would make the effects of quenching very difficult to detect by an integrated measurement of the emission from balloon altitudes. In an integrated measurement from a balloon (or ground) the effects on vibrational population from atomic oxygen quenching and a secondary source such as $HO_2 + O$ act in opposition; that is, quenching by atomic oxygen tends to reduce the emission from the lower vibrational levels, whereas $HO_2 + O$ tends to cause an increase. On the basis of the assumption of no atomic oxygen quenching and on the basis of rocket measurements with a single spectral band pass covering 1.65–1.89 μm and a radiometric measurement of O_2 ($^1\Delta_g$), *Evans and Llewelyn* [1973] further conclude that the H concentration is $3 \times 10^7 \text{ cm}^{-3}$ at 90 km. As they point out, this appears to be a value much lower than that predicted by a number of other investigators. If OH were quenched by atomic oxygen at higher altitudes, as is suggested by our measurements, then the H concentration could be adjusted upward by an order of magnitude, giving good agreement with theoretical models.

CONCLUSIONS

Simultaneous emission measurements of the upper and lower vibrational levels of OH have shown the OH emission to be concentrated in a layer at 83.5 km approximately 8 km in depth.

It is reasonably established that the upper vibrational levels ($v = 7, 8, 9$) of atmospheric OH are principally populated by the $H + O_3$ reaction. On the basis of this assumption, a theoretical spectrum of the vibrational-rotational bands of the first overtone of OH including complete cascading and no quenching was generated to predict the intensity of radiation due to the ozone reaction. A predicted intensity ratio between the two radiometers was derived by integrating this theoretical spectrum with the response of each data channel.

The predicted ratio was coincident with the measured ratio at approximately 82 km. Relative to the long-wavelength data channel the short-wavelength data channel had a larger emission below 82 km and a smaller emission above 82 km than was predicted. The relative decreased emission of the short-wavelength channel above 82 km is interpreted to indicate that the upper levels of OH are being quenched by atomic oxygen before they are able to cascade to the lower vibrational levels.

An atomic oxygen profile was determined by calculating the [O] necessary for quenching to be consistent with the measured OH volume emission rates. The derived oxygen concentration varies from 10^{11} cm^{-3} at 83 km to $8 \times 10^{11} \text{ cm}^{-3}$ at 88 km.

The atomic oxygen concentration agrees in magnitude and shape with the measurement of *Henderson* [1971] but is at an altitude approximately 7 km lower. The observed lowering of the atomic oxygen profile in the auroral zone is in accord with the conclusions of *Dandekar* [1972].

Acknowledgments. The authors are indebted to many workers, notably Clair Wyatt, Doran Baker, and John Kemp of Utah State University, as well as Ed McKenna and Ray Wilton of the AFCRL Aerospace Instrumentation Laboratory and personnel of the Geophysical Institute, University of Alaska.

The authors wish to acknowledge the support of the Defense Nuclear Agency (Atmospheric Effects Division), since this rocket experiment was one of the Ice Cap 72 launches, a program of coordinated experiments for understanding the physics and chemistry of the upper atmosphere at high latitudes.

REFERENCES

- Baker, D. J., and R. O. Waddoups, Rocket measurement of mid-latitude night airglow emissions, *J. Geophys. Res.*, **72**, 4881–4883, 1967.
- Bates, J. R., and B. L. Moiseiwitsch, Origin of the Meinel hydroxyl system in the airglow emissions, *J. Atmos. Terr. Phys.*, **8**, 305–308, 1956.

- Bunn, F. E., and H. P. Gush, Spectrum of the airglow between 3 and 4 microns, *Can. J. Phys.*, **50**, 213-215, 1972.
- Charters, P. E., R. G. MacDonald, and J. C. Polanyi, Formation of vibrationally excited OH by the reaction $H + O_3$, *Appl. Opt.*, **10**, 1747-1754, 1971.
- Dandekar, B. S., Atomic oxygen concentration from the [OI] 5577 A line emission at the auroral zone latitude, *Planet. Space Sci.*, **20**, 1781-1784, 1972.
- Evans, W. F. J., and E. J. Llewellyn, Excitation rates of the vibrational levels of hydroxyl and nightglow intensities, *Planet. Space Sci.*, **20**, 624-627, 1971.
- Evans, W. F. J., and E. J. Llewellyn, Atomic hydrogen concentrations in the mesosphere and the hydroxyl emissions, *J. Geophys. Res.*, **78**, 323-326, 1973.
- Gattinger, R. L., Interpretation of airglow emissions—OH emissions, *Ann. Geophys.*, **25**, 825-830, 1969.
- Gattinger, R. L., Interpretation of airglow in terms of excitation mechanisms, in *The Radiating Atmosphere*, edited by B. M. McCormac, pp. 51-63, D. Reidel, Dordrecht, Netherlands, 1971.
- Gush, H. P., and H. L. Buijs, The near infrared spectrum of the night airglow observed from high altitudes, *Can. J. Phys.*, **42**, 1037-1045, 1964.
- Harrison, A. W., Altitude profile of airglow hydroxyl emission, *Can. J. Phys.*, **48**, 2231-2234, 1971.
- Henderson, W. R., D-region atomic oxygen measurement, *J. Geophys. Res.*, **76**, 3166-3167, 1971.
- Huppi, R. J., K. D. Baker, and D. J. Baker, Ground-based auroral measurements during Ice Cap 72 program, scientific report, Dep. of Elec. Eng., Utah State Univ., Logan, Utah, 1973.
- Jensen, L. L., J. C. Kemp, and R. J. Bell, Small rocket instrumentation for measurements of infrared emissions, *Rep. 72-0691*, Air Force Cambridge Res. Lab., Bedford, Mass., 1972.
- Kaufman, F., Aeronomic reactions involving hydrogen, A review of recent laboratory studies, *Ann. Geophys.*, **20**, 106-114, 1964.
- Krassovsky, V. I., The hydroxyl emission problem and paths of its solution, *Ann. Geophys.*, **27**, 211-221, 1971.
- Krassovsky, V. I., N. N. Shefov, and V. I. Yarin, On the OH airglow, *J. Atmos. Terr. Phys.*, **21**, 46-53, 1961.
- Krassovsky, V. I., Rotational and vibrational hydroxyl excitation in the laboratory and in the night airglow, *J. Atmos. Terr. Phys.*, **35**, 705-711, 1973.
- Lowe, R. P., and E. A. Lytle, Balloon-borne spectroscopic observation of the infrared hydroxyl airglow, *Appl. Opt.*, **12**, 579-583, 1973.
- Murphy, R. E., Infrared emission of OH in the fundamental and first overtone bands, *J. Chem. Phys.*, **54**, 4852-4859, 1971.
- Packer, D. M., Altitudes of the night airglow radiations, *Ann. Geophys.*, **17**, 67-75, 1961.
- Pearce, J. B., Rocket measurements of nitric oxide between 60 and 95 kilometers, *J. Geophys. Res.*, **74**, 853-861, 1969.
- Shefov, N. N., Hydroxyl emissions of the upper atmosphere, *Planet. Space Sci.*, **19**, 129-136, 1971.
- Shefov, N. N., Hydroxyl emission, *Ann. Geophys.*, **28**, 137-143, 1972.
- Shimazaki, T., and A. R. Laird, A model calculation of the diurnal variation in minor neutral constituents in the mesosphere and lower thermosphere including transport effects, *J. Geophys. Res.*, **75**, 3221-3235, 1970.
- Sivjee, G. G., K. A. Dick, and P. D. Feldman, Temporal variations in nighttime hydroxyl rotational temperature, *Planet. Space Sci.*, **20**, 261-269, 1972.
- Stair, A. T., Jr., E. R. Huppi, B. S. Sandford, R. E. Murphy, R. R. O'Neil, A. M. Hart, R. J. Huppi, and W. R. Pendleton, Infrared investigations of the aurora and airglow, in *The Radiating Atmosphere*, edited by B. M. McCormac, pp. 185-204, D. Reidel, Dordrecht, Netherlands, 1971.
- Tarasova, T. M., Direct measurements of the night airglow in the spectral region $\lambda = 8640$ A, *Planet. Space Sci.*, **11**, 437-439, 1963.
- Worley, S. D., R. N. Coltharp, and A. E. Potter, Quenching of vibrationally excited hydroxyl ($v = 9$) with oxygen, *J. Chem. Phys.*, **55**, 2608-2609, 1971.
- Worley, S. D., R. N. Coltharp, and A. E. Potter, Rates of interaction of vibrationally excited hydroxyl ($v = 9$) with diatomic and small polyatomic molecules, *J. Phys. Chem.*, **76**, 1511-1514, 1972.

(Received March 30, 1973;
revised July 13, 1973.)